(m, 1, CH), 1.35 (s, 6, 2 CH_3), 1.56–1.66 (m, 1, CH), 1.77–1.89 (m, 1, CH), 1.95 (d, 1, $J = 4.4$ Hz, CH), 2.27 (br s, 7, 2 NCH_3 and NCH), 4.10 (d, 1, $J = 6.8$ Hz, C*H*OH); ^{13}C NMR (67.8 MHz, toluene-d_8) δ −14.15, 12.63, 22.46, 23.01, 29.66, 33.32, 44.07, 46.00, 47.95, 49.65, 50.29, 77.53, 85.28; mp >160 °C dec. With use of (±)-DAIB (1.10 g, 5.59 mmol), **11** was prepared in 81% yield: ^1H NMR (270 MHz, toluene-d_8) δ −0.28 (s, 3, $ZnCH_3$), 0.93 (s, 3, CH_3), 0.91–1.01 (m, 1, CH), 1.15–1.34 (m, 1, CH), 1.25 (s, 3, CH_3), 1.39 (s, 3, CH_3), 1.53–1.65 (m, 1, CH), 1.74–1.86 (m, 1, CH), 1.92 (d, 1, $J = 4.9$ Hz, CH), 2.26 (s, 3, NCH_3), 2.29 (d, 1, $J = 6.8$ Hz, NCH), 2.46 (s, 3, NCH_3), 4.29 (d, 1, $J = 6.8$ Hz, C*H*OH); ^{13}C NMR (67.8 MHz, toluene-d_8) δ −16.57, 12.00, 22.66, 23.35, 29.68, 33.36, 44.39, 45.93, 48.23, 49.87, 50.70, 78.27, 84.35; mp >180 °C dec.

X-ray Analysis of the Complexes (−)(−)-1 and 11 (R = CH_3). Single crystals of (−)(−)-**1** and **11** suitable for diffraction experiments were obtained by recrystallization from toluene and benzene at room temperature. The crystals were sealed in thin-walled capillary tubes (Oversees X-ray Service Co., 0.3 mm i.d. for (−)(−)-**1** and 0.7 mm i.d. for **11**) in a glovebox. Crystallographic data, data collection details, data reduction and refinement details for (−)(−)-**1** and **11** are summarized in Table IV. Selected interatomic distance and angles are listed in Table V for (−)(−)-**1** and in Table VI for **11**. ORTEP drawings of (−)(−)-**1** and **11** with the numbering scheme are shown in Figures 6 and 7, respectively.

Acknowledgment. We thank A. Kawamoto, Nagoya University, for his valuable contribution in the X-ray crystallographic analyses. This work was aided by Grant-in-Aid for Specially Promoted Research (No. 62065005) from the Ministry of Education, Science and Culture of Japan.

Supplementary Material Available: Tables of atomic parameters, anisotropic temperature factors, and bond angles and distances for (−)(−)-**1** and **11** (48 pages); complete listings of observed and calculated structure factors for (−)(−)-**1** and **11** (12 pages). Ordering information is given on any current masthead page.

Sulfur–Sulfur Lone Pair and Sulfur–Naphthalene Interactions in Naphtho[1,8-*b*,*c*]-1,5-dithiocin

Richard S. Glass,* Stephen W. Andruski, Jeffrey L. Broeker, Habib Firouzabadi,[†] L. Kraig Steffen, and George S. Wilson[‡]

Contribution from the Department of Chemistry, University of Arizona, Tucson, Arizona 85721. Received September 12, 1988

Abstract: Naphtho[1,8-*b*,*c*]-1,5-dithiocin (**4**), which has a unique geometry so constrained that the sulfur atoms are held close to one another and oriented such that their p orbitals are almost colinear and orthogonal to the naphthalene π-system, has been synthesized. Its crystal and molecular structure was determined by single-crystal X-ray analysis. It crystallizes in the orthorhombic space group *Pbca* with $a = 8.140$ (2) Å, $b = 9.866$ (1) Å, $c = 28.302$ (3) Å, and $Z = 8$. The structure was solved by direct methods. Full-matrix least-squares refinement led to a conventional *R* factor of 0.046 after several cycles of anisotropic refinement. For comparison purposes the crystal and molecular structure of the previously reported 1,8-bis(methylthio)naphthalene (**5**) was also determined by X-ray techniques. Semiempirical molecular orbital methods (MNDO and AM1) were used to analyze the five highest occupied molecular orbitals in 1,8-bis(methylthio)naphthalene as a function of the C(1)–S and C(8)–S torsion angles and to analyze the molecular orbitals of compound **4**. Of particular interest is the result that the energy of the highest occupied molecular orbital in 1,8-bis(methylthio)naphthalene is nearly independent of the C–S torsion angle and that the lowest ionization potential for **4** is predicted to be 7.75 eV and its lone pair–lone pair splitting due to transannular S–S interaction is 1.6–2.0 eV. The computations were correlated with the experimentally measured He I and He II photoelectron spectra of **4** and the AM1 method provided reasonable agreement with the experimental data. The electrochemical oxidation of **4** and **5** in acetonitrile was studied by cyclic voltammetry. They undergo irreversible oxidation with peak potentials of 0.70 and 0.47 V, respectively, versus a Ag/0.1 M $AgNO_3$ in acetonitrile reference electrode. Controlled-potential electrolysis of **4** gives the corresponding sulfoxide (**12**), which is consistent with removal of an electron from the highest occupied molecular orbital which is sulfur lone pair in character.

Oxidation of 1,5-dithiocane, **1**, to the corresponding, unusually stable, radical cation **2**[1-4] and dication **3**[2,3,5] occurs with remarkable ease. The peak potential for this reversible oxidation is 0.34 V in acetonitrile versus a Ag/$AgNO_3$ in acetonitrile reference electrode.[6,7] This oxidation can also be achieved chemically.[1,2] The basis for this facile oxidation has been ascribed to the destabilization of 1,5-dithiocane, **1**, by transannular lone-pair–lone-pair repulsion and the stabilization of the oxidized products by neighboring-group participation, that is, bond formation between the two sulfur atoms. The bonding between the sulfur atoms in the radical cation of 1,5-dithiocane has been convincingly established[8,9] as $\sigma^2\sigma^{*1}$ and a chemical consequence of this bonding is the unusual ease of removal of a second electron from 1,5-

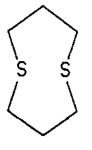

1

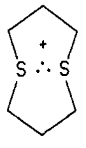

2

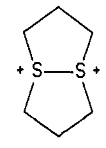

3

[†] On leave from the Department of Chemistry, Shiraz University, Shiraz, Iran.

[‡] Present address: Department of Chemistry, University of Kansas, Lawrence, KS 66045.

(1) Musker, W. K.; Wolford, T. L. *J. Am. Chem. Soc.* **1976**, *98*, 3055.
(2) Musker, W. K.; Wolford, T. L.; Roush, P. B. *J. Am. Chem. Soc.* **1978**, *100*, 6416.
(3) Musker, W. K. *Acc. Chem. Res.* **1980**, *13*, 200.
(4) Brown, T. G.; Hirschon, A. S.; Musker, W. K. *J. Phys. Chem.* **1981**, *85*, 3767.
(5) Musker, W. K.; Roush, P. B. *J. Am. Chem. Soc.* **1976**, *98*, 6745.
(6) Wilson, G. S.; Swanson, D. D.; Klug, J. T.; Glass, R. S.; Ryan, M. D.; Musker, W. K. *J. Am. Chem. Soc.* **1979**, *101*, 1040.
(7) Ryan, M. D.; Swanson, D. D.; Glass, R. S.; Wilson, G. S. *J. Phys. Chem.* **1981**, *85*, 1069.
(8) Asmus, K.-D.; Bahnemann, D.; Fischer, Ch.-H.; Veltwisch, D. *J. Am. Chem. Soc.* **1979**, *101*, 5322.
(9) Asmus, K.-D. *Acc. Chem. Res.* **1979**, *12*, 436.

0002-7863/89/1511-4036$01.50/0 © 1989 American Chemical Society

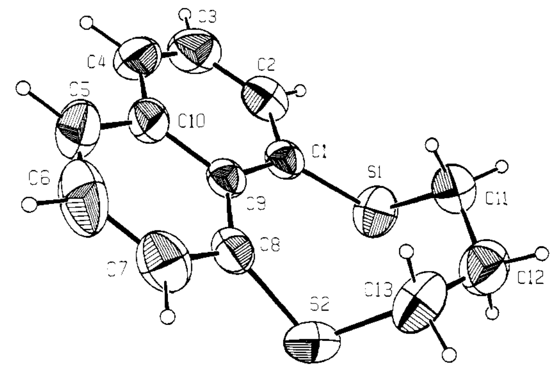

Figure 1. ORTEP[65] drawing of naphtho[1,8-*b*,*c*]-1,5-dithiocin (**4**) and the labeling scheme. Thermal ellipsoids are drawn at the 50% probability level.

dithiocane, i.e. the antibonding electron in the radical cation, resulting in $E_1^{0\prime}$ being slightly more positive than $E_2^{0\prime}$ for this compound.[6,7] Such effects might be enhanced in conformationally constrained derivatives of **1** such as naphtho[1,8-*b*,*c*]-1,5-dithiocin, **4**. Owing to the geometry and rigidity of the naphthalene ring, the sulfur atoms, which are in the so-called "peri" position,[10] are close to one another in this compound and the p-type lone pair orbitals on sulfur are directed at each other. These two factors should ensure augmented lone-pair–lone-pair interaction.[11] This paper presents the synthesis, crystal and molecular structure determined by X-ray methods, photoelectron spectra, computational studies, and electrochemistry of **4**. In addition, the crystal and molecular structure determined by X-ray methods and computational studies of 1,8-bis(methylthio)naphthalene **5**[12] are included for comparison.

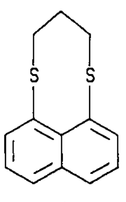

4

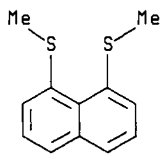

5

Results and Discussion

Synthesis. Synthesis of naphtho[1,8-*b*,*c*]-1,5-dithiocin, **4**, by alkylation of the known 1,8-naphthalenedithiol, **6**,[12] using a variety of conditions[13,14] provided **4** irreproducibly in, at best, 45% yield.

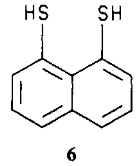

6

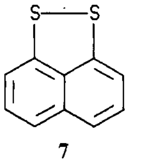

7

However, **4** was prepared in very good yield from naphtho[1,8-*c*,*d*]-1,2-dithiole,[12] **7**, by using the procedure of Ferreira et al.[15] In this method the disulfide is reduced under weakly aqueous alkaline conditions with aminoiminomethanesulfinic acid and alkylated under phase-transfer conditions. In this way, pure crystalline **4** was made reproducibly in 85% yield.

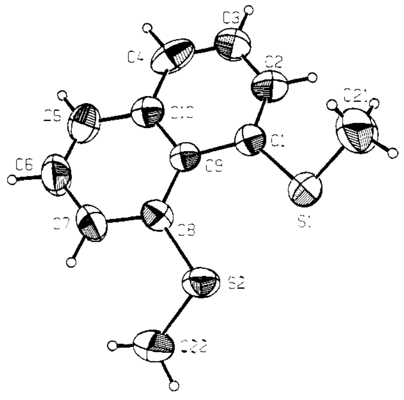

Figure 2. ORTEP[65] drawing of 1,8-bis(methylthio)naphthalene (**5**) of independent molecule 1 with the labeling scheme. Thermal ellipsoids are drawn at the 50% probability level.

Table I. Bond Distances for Non-Hydrogen Atoms in **4**[a]

atoms	distance, Å	atoms	distance, Å
S1-C1	1.764 (4)	S1-C11	1.814 (4)
S2-C8	1.779 (4)	S2-C13	1.817 (4)
C1-C2	1.379 (5)	C1-C9	1.436 (4)
C2-C3	1.389 (6)	C3-C4	1.331 (6)
C4-C10	1.401 (5)	C5-C6	1.345 (6)
C5-C10	1.403 (5)	C6-C7	1.393 (6)
C7-C8	1.368 (5)	C8-C9	1.438 (5)
C9-C10	1.445 (5)	C11-C12	1.495 (6)
C12-C13	1.492 (6)		

[a] Numbers in parentheses are estimated standard deviations in the least significant digits.

Table II. Bond Angles for Non-Hydrogen Atoms in **4**[a]

atoms	angle, deg	atoms	angle, deg
C1-S1-C11	104.3 (2)	C8-S2-C13	104.5 (2)
S1-C1-C2	113.4 (3)	S1-C1-C9	127.0 (3)
C2-C1-C9	119.6 (3)	C1-C2-C3	122.4 (3)
C2-C3-C4	119.9 (4)	C3-C4-C10	121.2 (4)
C6-C5-C10	120.8 (4)	C5-C6-C7	120.2 (4)
C6-C7-C8	122.3 (4)	S2-C8-C7	114.1 (3)
S2-C8-C9	126.0 (3)	C7-C8-C9	119.5 (3)
C1-C9-C8	127.4 (3)	C1-C9-C10	115.8 (3)
C8-C9-C10	116.7 (3)	C4-C10-C5	118.8 (4)
C4-C10-C9	120.9 (3)	C5-C10-C9	120.3 (3)
S1-C11-C12	114.4 (3)	C11-C12-C13	115.0 (4)
S2-C13-C12	115.4 (3)		

[a] Numbers in parentheses are estimated standard deviations in the least significant digits.

Table III. Selected Torsion Angles for **4**

atoms	angle, deg	atoms	angle, deg
C11-S1-C1-C2	114.7	C11-S1-C1-C9	-68.0
C1-S1-C11-C12	112.4	C13-S2-C8-C7	-100.5
C13-S2-C8-C9	86.5	C8-S2-C13-C12	-100.8
S1-C1-C2-C3	178.0	C9-C1-C2-C3	0.5
S1-C1-C9-C8	-1.0	S1-C1-C9-C10	179.3
C2-C1-C9-C8	176.2	C2-C1-C9-C10	-3.5
C1-C2-C3-C4	2.1	C2-C3-C4-C10	-1.4
C3-C4-C10-C5	179.7	C3-C4-C10-C9	-1.9
C10-C5-C6-C7	-2.8	C6-C5-C10-C4	178.6
C6-C5-C10-C9	0.1	C5-C6-C7-C8	2.3
C6-C7-C8-S2	-172.6	C6-C7-C8-C9	1.0
S2-C8-C9-C1	-10.4	S2-C8-C9-C10	169.2
C7-C8-C9-C1	176.9	C7-C8-C9-C10	-3.5
C1-C9-C10-C4	4.3	C1-C9-C10-C5	-177.3
C8-C9-C10-C4	-175.4	C8-C9-C10-C5	3.0
S1-C11-C12-C13	-75.5	C11-C12-C13-S2	65.1

The structure and conformation of **4** in the solid state was unequivocally established by X-ray methods. The structure and conformation in the solid state of the known[12] 1,8-bis(methylthio)naphthalene was also determined by single-crystal X-ray techniques for comparison purposes.

X-ray Crystal Structure Studies. ORTEP drawings of naphtho[1,8-*b*,*c*]-1,5-dithiocin, **4**, and 1,8-bis(methylthio)-

---

(10) Balasubramaniyan, V. *Chem. Rev.* **1966**, *66*, 567.

(11) Setzer, W. N.; Coleman, B. R.; Wilson, G. S.; Glass, R. S. *Tetrahedron* **1981**, *37*, 2743.

(12) Zweig, A.; Hoffmann, A. K. *J. Org. Chem.* **1965**, *30*, 3997.

(13) Setzer, W. N.; Ogle, C. A.; Wilson, G. S.; Glass, R. S. *Inorg. Chem.* **1983**, *22*, 266.

(14) Buter, J.; Kellogg, R. M. *J. Org. Chem.* **1981**, *46*, 4481.

(15) Ferreira, J. T. B.; Simonelli, F.; Comasseto, J. V. *Synth. Commun.* **1986**, *16*, 1335.

Table IV. Bond Distances for Non-Hydrogen Atoms in **5**[a]

atoms	distance, Å	atoms	distance, Å
	Molecule 1		
S1–C1	1.785 (4)	S2–C8	1.778 (4)
S1–C21	1.778 (5)	S2–C22	1.762 (5)
C1–C2	1.378 (6)	C1–C9	1.433 (5)
C2–C3	1.391 (6)	C3–C4	1.353 (7)
C4–C10	1.397 (6)	C5–C6	1.349 (7)
C5–C10	1.416 (6)	C6–C7	1.377 (6)
C7–C8	1.380 (6)	C8–C9	1.436 (5)
C9–C10	1.430 (5)		
	Molecule 2		
S3–C11	1.774 (4)	S3–C23	1.793 (5)
S4–C18	1.768 (4)	S4–C24	1.772 (5)
C11–C12	1.341 (5)	C11–C19	1.463 (5)
C12–C13	1.385 (6)	C13–C14	1.363 (7)
C14–C20	1.409 (6)	C15–C16	1.332 (6)
C15–C20	1.433 (6)	C16–C17	1.411 (6)
C17–C18	1.411 (6)	C18–C19	1.420 (5)
C19–C20	1.417 (5)		

[a] The numbers in parentheses are estimated standard deviations in the least significant digits.

Table V. Bond Angles for Non-Hydrogen Atoms in **5**[a]

atoms	angle, deg	atoms	angle, deg
	Molecule 1		
S1–C1–C2	117.5 (4)	S1–C1–C9	122.5 (3)
C2–C1–C9	120.0 (4)	C1–C2–C3	122.1 (5)
C2–C3–C4	119.7 (5)	C3–C4–C10	120.4 (5)
C6–C5–C10	121.2 (4)	C5–C6–C7	120.5 (5)
C6–C7–C8	122.0 (5)	S2–C8–C7	119.6 (3)
S2–C8–C9	121.1 (3)	C7–C8–C9	119.2 (4)
C1–C9–C8	126.3 (4)	C1–C9–C10	115.9 (4)
C8–C9–C10	117.8 (4)	C4–C10–C5	119.1 (4)
C4–C10–C9	121.7 (4)	C5–C10–C9	119.1 (4)
C1–S1–C21	104.0 (2)	C8–S2–C22	103.6 (2)
	Molecule 2		
C11–S3–C23	101.6 (2)	C18–S4–C24	103.2 (2)
S3–C11–C12	119.1 (3)	S3–C11–C19	122.1 (3)
C12–C11–C19	118.8 (4)	C11–C12–C13	124.6 (5)
C12–C13–C14	118.4 (4)	C13–C14–C20	120.6 (4)
C16–C15–C20	120.5 (4)	C15–C16–C17	120.5 (4)
C16–C17–C18	120.9 (4)	S4–C18–C17	117.4 (3)
S4–C18–C19	123.5 (3)	C17–C18–C19	119.0 (4)
C11–C19–C18	125.4 (4)	C11–C19–C20	116.2 (3)
C18–C19–C20	118.4 (4)	C14–C20–C15	118.6 (4)
C14–C20–C19	121.2 (4)	C15–C20–C19	120.2 (4)

[a] The numbers in parentheses are standard deviations in the least significant digits.

Table VI. Selected Torsion Angles for **5**

atoms	angle, deg	atoms	angle, deg
	Molecule 1		
S1–C1–C2–C3	−173.8	C9–C1–C2–C3	3.3
S1–C1–C9–C8	−8.3	S1–C1–C9–C10	171.8
C2–C1–C9–C8	174.7	C2–C1–C9–C10	−5.1
C1–C2–C3–C4	0.6	C2–C3–C4–C10	−2.3
C3–C4–C10–C5	179.7	C3–C4–C10–C9	0.2
C10–C5–C6–C7	−1.2	C6–C5–C10–C4	179.6
C6–C5–C10–C9	−0.9	C5–C6–C7–C8	0.0
C6–C7–C8–S2	−172.9	C6–C7–C8–C9	3.4
S2–C8–C9–C1	−8.9	S2–C8–C9–C10	170.9
C7–C8–C9–C1	174.8	C7–C8–C9–C10	−5.3
C1–C9–C10–C4	3.5	C1–C9–C10–C5	−176.0
C8–C9–C10–C4	−176.4	C8–C9–C10–C5	4.1
C21–S1–C1–C2	33.8	C21–S1–C1–C9	−143.2
C22–S2–C8–C7	17.9	C22–S2–C8–C9	−158.3
	Molecule 2		
C23–S3–C11–C12	38.1	C23–S3–C11–C19	−142.0
C24–S4–C18–C17	24.3	C24–S4–C18–C19	−153.0
S3–C11–C12–C13	−175.2	C19–C11–C12–C13	4.9
S3–C11–C19–C18	−6.4	S3–C11–C19–C20	174.4
C12–C11–C19–C18	173.5	C12–C11–C19–C20	−5.7
C11–C12–C13–C14	−0.6	C12–C13–C14–C20	−2.7
C13–C14–C20–C15	−177.8	C13–C14–C20–C19	1.5
C16–C15–C20–C14	−177.2	S4–C18–C19–C11	−7.6
S4–C18–C19–C20	171.7	C17–C18–C19–C11	175.1
C17–C18–C19–C20	−5.7	C11–C19–C20–C14	2.7
C11–C19–C20–C15	−178.0	C18–C19–C20–C14	−176.6
C18–C19–C20–C15	2.7	C16–C15–C20–C19	3.5
C15–C16–C17–C18	3.4	C16–C17–C18–S4	−174.6
C16–C17–C18–C19	2.9		

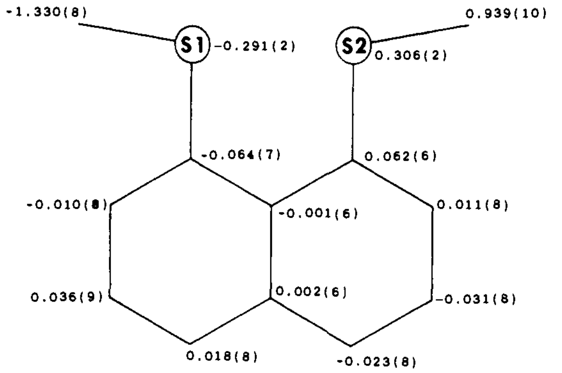

Figure 3. Deviations from the least-squares plane of the naphthalene ring in **5**. Numbers in parentheses are estimated standard deviations in the least significant digits.

naphthalene, **5**, and the labeling schemes used are shown in Figures 1 and 2, respectively. Tables of bond lengths, bond angles, and selected torsional angles for each of the compounds are given in Tables I–VI. The naphthalene ring in compound **5** is slightly twisted about the C(9)–C(10) axis and the sulfur atoms are displaced above and below the average plane of the naphthalene ring by almost 0.3 Å as shown in Figure 3. The twisting of the naphthalene ring is symmetric within experimental error and the displacement of the sulfur atoms nearly so. More substantial twisting of the naphthalene ring has been observed in 1,8-disubstituted derivatives with bulky substituents.[16,17] The nonbonded S···S distance is 2.93 Å (average of molecules 1 and 2, 2.918 (2) and 2.934 (2) Å, respectively), whereas twice the van der Waals radius of sulfur is 3.70 Å.[18] Although S···S nonbonded distances of less than 3.70 Å have been reported,[19,20] the value here is unusually short. In order to relieve steric interaction between the methylthio groups and the ortho hydrogen atoms, there is rotation about the C(1)–S and C(8)–S bonds. An alternate way to relieve this steric interaction, which is illustrated in the crystal structure[21] of the cardiotonic drug 2-[(2-methoxy-4-(methylthio)phenyl]-1*H*-imidazo[4,5-*b*]pyridine, **8**, is to open the S–C–C angle on the side of the methyl group. This angle is 125.2° in compound **8**. However, such distortion would decrease the S···S distance in **5** and increase the repulsive "peri" steric interaction. Thus the average S–C–C angles in **5** are 118.4° and there is rotation about C(1)–S and C(8)–S. Both bonds are rotated in the same sense

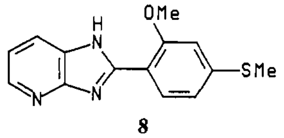

8

---

(16) Robert, J.-B.; Sherfinski, J. S.; Marsh, R. E.; Roberts, J. D. *J. Org. Chem.* **1974**, *39*, 1152 and references therein.

(17) Schweizer, W. B.; Proctor, G.; Kaftory, M.; Dunitz, J. D. *Helv. Chim. Acta* **1978**, *61*, 2783.

(18) Pauling, L. In *The Nature of the Chemical Bond*, 3rd ed.; Cornell: Ithaca, 1960, p 260.

(19) Guru Row, T. N.; Parthasarathy, R. *J. Am. Chem. Soc.* **1981**, *103*, 477.

(20) Glass, R. S.; Coleman, B. R.; Prabhu, U. D. G.; Setzer, W. N.; Wilson, G. S. *J. Org. Chem.* **1982**, *47*, 2761.

(21) Luger, P.; Rabius, E.; Kutter, E.; Austel, V. *Acta Crystallogr.* **1987**, *C43*, 1937.

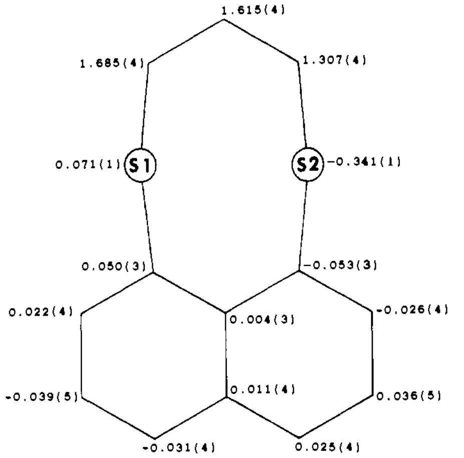

Figure 4. Deviations from the least-squares plane of the naphthalene ring in **4**. Numbers in parentheses are estimated standard deviations in the least significant digits.

Table VII. Asymmetry Parameters for the Dithiocin Ring of **4**[a]

$\Delta C_s(\mathrm{S1}) = 0.161\ (1)$	$\Delta C_s(\mathrm{S1{-}C11}) = 0.443\ (1)$
$\Delta C_2(\mathrm{S1}) = 0.346\ (1)$	$\Delta C_2(\mathrm{S1{-}C11}) = 0.262\ (1)$
$\Delta C_s(\mathrm{C1}) = 0.474\ (1)$	$\Delta C_s(\mathrm{C1{-}S1}) = 0.375\ (1)$
$\Delta C_2(\mathrm{C1}) = 0.269\ (1)$	$\Delta C_2(\mathrm{C1{-}S1}) = 0.352\ (1)$
$\Delta C_s(\mathrm{C9}) = 0.081\ (1)$	$\Delta C_s(\mathrm{C9{-}C1}) = 0.455\ (1)$
$\Delta C_2(\mathrm{C9}) = 0.445\ (1)$	$\Delta C_2(\mathrm{C9{-}C1}) = 0.239\ (1)$
$\Delta C_s(\mathrm{C8}) = 0.476\ (1)$	$\Delta C_s(\mathrm{C8{-}C9}) = 0.388\ (1)$
$\Delta C_2(\mathrm{C8}) = 0.246\ (1)$	$\Delta C_2(\mathrm{C8{-}C9}) = 0.338\ (1)$

[a] The numbers in parentheses are estimated standard deviations in the least significant digits.

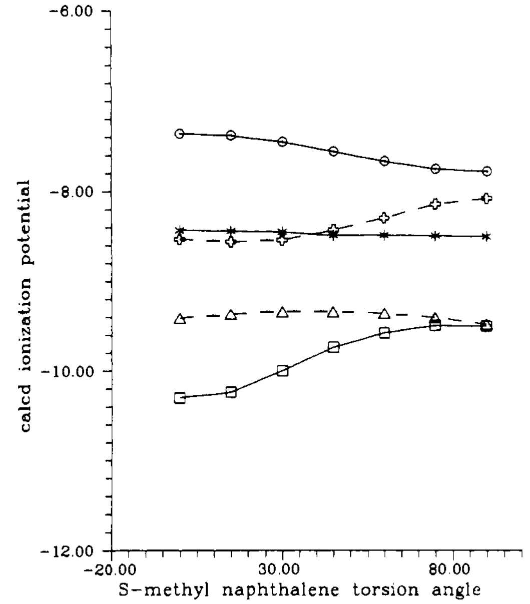

Figure 5. Dependence of the ionization potentials of the five highest occupied molecular orbitals of 1,8-bis(methylthio)naphthalene (**5**) on the C(1)-S and C(8)-S torsion angles as calculated by the MNDO method. IPs were calculated from the equation: IP = −1.031(ϵ_j) − 1.402, where IP = ionization potential and ϵ_j = eigenvalue. This equation was obtained by correlating the experimental IPs of 1,8-bis(methylthio)naphthalene with the calculated eigenvalues at the 30° torsion angle.

(conrotatory) although not symmetrically. The average rotation angle is 28.5°. The major axis of the p-type orbital on each of the sulfur atoms is rotated away from that of the π-system of the naphthalene ring, but there is still overlap[22] between the sulfur and π-orbitals and the sulfur p-type orbitals are roughly parallel to each other.

There is also a small twisting about the C(9)–C(10) axis of the naphthalene ring in compound **4** with the sulfur atoms asymmetrically disposed above and below the average plane of the naphthalene ring as shown in Figure 4. The nonbonded S···S distance in this compound is 3.227 (1) Å. The S(1)–C(1)–C(9) and S(2)–C(8)–C(9) bond angles in this compound are approximately 5° larger than the corresponding angles in **5**. The C(1)–C(9)–C(8) angle in **4** is also slightly larger than the corresponding angle in **5** (by 1.6° over the average of that in molecules 1 and 2 of **5**). As pointed out for compound **5**, there is rotation about the C(1)–S and C(8)–S bonds. In a similar way, the geometry of **4** can be described by such rotation. In order to form the eight-membered ring in **4**, the sense of the rotations must be opposite (disrotatory). This rotation is not symmetric about C(1)–S(1) and C(8)–S(2), but the average rotation is 82°. Thus the major axis of the p-type orbital on each of the sulfur atoms are approaching colinearity with each other and orthogonality with that of the naphthalene π-system.[23] It has been suggested[19,24-28] that the nonbonded-electron density about a sulfur atom is not spherically symmetrical because one electron pair is in a p-type orbital and the other in a hybrid orbital. There is a greater extension of electron density perpendicular to the C–S–C plane (along the major axis of the p orbital) than in the C–S–C plane. The greater S···S nonbonded distance in **4** than **5** and greater S(1)–C(1)–C(9), S(2)–C(8)–C(9), and C(1)–C(9)–C(8) angles in **4** than the corresponding angles in **5** are in accord with this suggestion.

The conformation of the eight-membered ring in **4** is of interest.[29-37] Owing to the 1,8-fusion to the naphthalene ring, S(1), C(1), C(8), and S(2) are approximately coplanar and a chair conformation with an approximate mirror plane through C(9) and C(12) is adopted. A more exact description of the conformation of this ring is given by the asymmetry parameters[38,39] shown in Table VII or by the ring puckering parameters[39,40] q_2 = 1.071 (3) Å, q_3 = 0.333 (4) Å, q_4 = 0.724 (3) Å, ϕ_2 = −9.3 (2)°, ϕ_3 = −93.1 (5)°, Q_t = 1.334 (2) Å, θ_2 = 72.7 (2)°, θ_3 = 24.7 (3)°. The S–C–C and C–C–C angles are all larger than tetrahedral angles.

The crystal structure data on naphtho[1,8-*b*,*c*]-1,5-dithiocin, **4**, clearly reveals that the sulfur atoms are close to each other and

---

(22) The average rotation angle about C(1)–S and C(8)–S with respect to the average plane of the naphthalene ring is 28.5°. However, the average torsion angle about C(1)–S, i.e., C(2)–C(1)–S(1)–C(21) and C(9)–C(1)–S(1)–C(21) average torsion angles, and C(8)–S, i.e., C(7)–C(8)–S(2)–C(12) and C(9)–C(8)–S(2)–C(12) average torsion angles, is 25° and this average angle may be more relevant for discerning the overlap between the sulfur p and carbon π-orbitals.

(23) The average rotation angle about C(1)–S and C(8)–S with respect to the average plane of the naphthalene ring is 82°. However, the average torsion angle about C(1)–S, i.e., C(2)–C(1)–S(1)–C(11) and C(9)–C(1)–S(1)–C(11) average torsion angle, and C(8)–S, i.e., C(7)–C(8)–S(2)–C(13) and C(9)–C(8)–S(2)–C(13) average torsion angles, is 75° and this average angle may be more relevant for discerning the geometric relationship between the sulfur p and carbon π-orbitals.

(24) Coppens, P.; Yang, Y. W.; Blessing, R. H.; Cooper, W. F.; Larsen, F. K. *J. Am. Chem. Soc.* **1977**, *99*, 760.

(25) Salahub, D. R.; Foti, A. E.; Smith, V. H., Jr. *J. Am. Chem. Soc.* **1977**, *99*, 8067.

(26) Rosenfield, R. E., Jr.; Parthasarathy, R.; Dunitz, J. D. *J. Am. Chem. Soc.* **1978**, *99*, 4860.

(27) Boyd, D. B. *J. Phys. Chem.* **1978**, *82*, 1407.

(28) Gleiter, R.; Spanget-Larsen, J. *Top. Curr. Chem.* **1979**, *86*, 139.

(29) Nelsen, S. F.; Gillespie, J. P. *J. Am. Chem. Soc.* **1973**, *95*, 2940.

(30) Kamada, T.; Yamamoto, O. *Chem. Lett.* **1976**, 843.

(31) Kamada, T.; Yamamoto, O. *Tetrahedron Lett.* **1977**, 691.

(32) Kamada, T.; Yamamoto, O. *Bull. Chem. Soc. Jpn.* **1979**, *52*, 1159.

(33) Kamada, T.; Yamamoto, O. *Bull. Chem. Soc. Jpn.* **1979**, *52*, 2991.

(34) Kamada, T.; Yamamoto, O. *Bull. Chem. Soc. Jpn.* **1980**, *53*, 994.

(35) Litvinov, I. A.; Klimovitskii, E. N.; Yufit, D. S.; Sergeeva, G. N.; Struchkov, Yu. T.; Arbuzov, B. A. *Proc. Acad. Sci. U.S.S.R., Chem. Sect.* **1981**, 115.

(36) Guttenberger, H. G.; Bestmann, H. J.; Dickert, F. L.; Jorgensen, F. S.; Snyder, J. P. *J. Am. Chem. Soc.* **1981**, *103*, 159.

(37) Arbuzov, B. A.; Klimovitskii, E. N.; Sergeeva, G. N.; Remizov, A. B.; Chernov, P. P. *J. Gen. Chem. USSR (Engl. Transl.)* **1983**, *53*, 2497.

(38) Nardelli, M. *Acta Crystallogr.* **1983**, *C39*, 1141.

(39) These parameters were calculated with the PARST program: Nardelli, M. *Comput. Chem.* **1983**, *7*, 95.

(40) Cremer, D.; Pople, J. A. *J. Am. Chem. Soc.* **1975**, *97*, 1354.

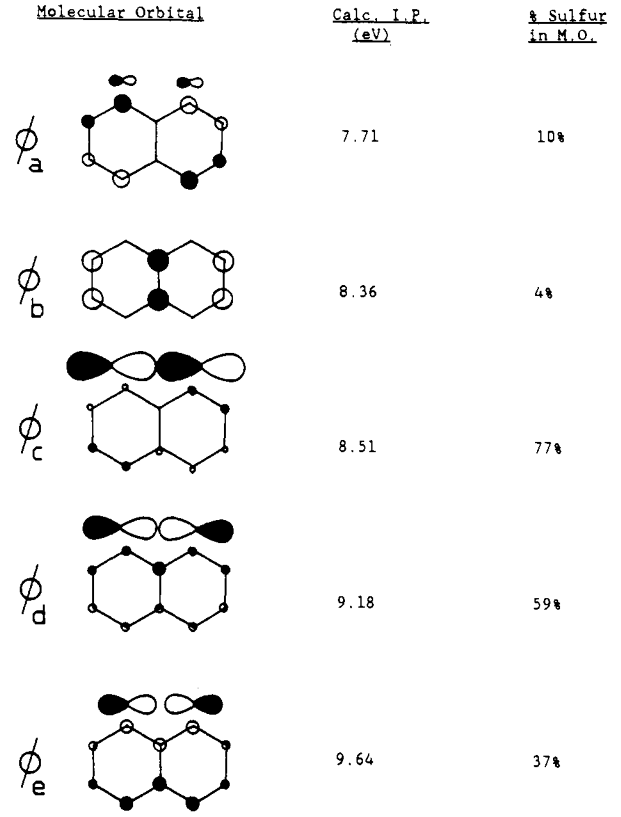

Figure 6. Orbital composition of the five highest occupied molecular orbitals for the optimized geometry of **4** as calculated by the MNDO method.

oriented for extensive lone pair–lone pair interaction. To quantitatively assess this interaction the photoelectron spectrum of this compound was measured and interpreted by comparison with computational results.

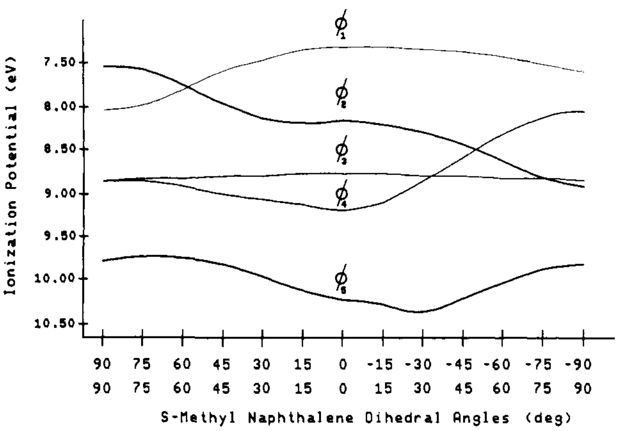

Figure 7. Dependence of the ionization potentials of the five highest occupied molecular orbitals of 1,8-bis(methylthio)naphthalene (**5**) on the C(1)–S and C(8)–S torsion angles as calculated by the AM1 method. Conrotation about C(1)–S and C(8)–S is designated +,+ and disrotation about these bonds is denoted by +,−. IPs were calculated from the equation: $\mathrm{IP} = -1.008(\epsilon_j) - 0.914$, where IP = ionization potential and ϵ_j = eigenvalue. This equation was obtained in a similar manner to that described in Figure 5.

Photoelectron Spectroscopy and Computations. The photoelectron spectrum of **5** was measured by Bock and Brähler[41] and our spectrum is in accord with their reported spectrum.[42] These workers also analyzed this spectrum by comparison with those of model compounds and semiempirical molecular orbital calculations with the CNDO program. They calculated the orbital energies for the five filled molecular orbitals of highest energy as a function of conrotation about the C(1)–S and C(8)–S bonds. The best fit between the calculated orbital energies and the measured ionization potentials, assuming Koopmans' theorem, was that for C–S torsion angles of 45°. This value is somewhat greater than that found in the solid state, which averaged 30° as presented above. With this analysis, at a dihedral angle of 90° the lowest ionization potential would be approximately 6.5 eV and the sulfur lone pair splitting would be 3.2 eV. Although the actual C–S torsion angles for **4** in the solid state average 82°,[23] the predictions for 90° should be approximately correct. However, CNDO/2 has been shown to not account properly for nonbonded interactions between oxygen, nitrogen,[43] or sulfur[27] atoms. Since it was expected that such interactions would be important in **4** (indeed, **4** was designed to insure substantial sulfur–sulfur lone pair interaction), MNDO calculations[44] were carried out in a similar manner as those reported with the CNDO program. Specifically, orbital energies are calculated as a function of conrotary rotation about the C(1)–S and C(8)–S bonds. The results for the five filled molecular orbitals of highest energy are shown in Figure 5. MNDO calculations with geometry optimization were carried out for **4** and the calculated geometry is similar to that determined by X-ray methods on a crystal of **4** except that the nonbonded S···S distance is shorter in the MNDO calculations than that found in the solid state (3.14 Å versus 3.23 Å). The orbital compositions for compound **4** as well as their corresponding first five ionization potentials (7.17, 8.36, 8.51, 9.18, and 9.64 eV) obtained from these MNDO calculations on compound **4** are shown in Figure 6. The ionization potentials were calculated from the eigenvalues of the first five HOMOs of compound **4** with the equation given in the caption of Figure 5. The sulfur–sulfur lone pair splitting is 0.9 eV. Further analysis was not done by using the MNDO method because it overestimates the repulsion between atoms at approximately their van der Waals' distances.[44-46] Owing to the likely importance of steric congestion in compound **4**, there is concern about the reliability of these calculations for this compound. Furthermore, the AM1 (Austin Model 1)[46] semiempirical method recently became available and it overcomes the problem with calculations on crowded molecules inherent in MNDO and it also uses an updated version of sulfur parameters.[47] Consequently, detailed analysis of compounds **4** and **5** were carried out by using AM1 as outlined below. The computed dependence of the five lowest ionization potentials on the C–S torsion angles of compound **5** both for conrotation and disrotation is illustrated in Figure 7.

A surprising feature of the AM1 calculations, illustrated in Figure 7, is that the lowest ionization potential is nearly the same regardless of the C–S torsion angles. This independence of the energy of the highest occupied molecular orbital on the C–S torsion angle was investigated by separating sulfur–sulfur lone pair interactions from sulfur lone pair–π interactions since both contribute to the highest occupied molecular orbital. Thus, AM1 calculations were done on hydrogen sulfide dimer **9** and (methylthio)naphthalene, **10**. The sulfur atoms of the two hydrogen sulfide molecules in dimer **9** were constrained to be the same

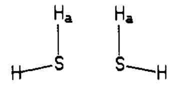

9

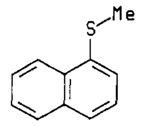

10

---

(41) Bock, H.; Brähler, G. *Chem. Ber.* **1979**, *112*, 3081.

(42) The published spectrum[41] and our spectrum for **5** are virtually superimposable. The reported five lowest ionization potentials are 7.55, 8.17, 8.76, and 10.08 eV. Our measured vertical ionization potentials are 7.42, 8.15, 8.75, 9.00, and 10.07 eV.

(43) Gregory, A. R.; Paddon-Row, M. N. *J. Am. Chem. Soc.* **1976**, *98*, 7521.

(44) Dewar, M. J. S.; Thiel, W. *J. Am. Chem. Soc.* **1977**, *99*, 4899, 4907.

(45) Dewar, M. J. S.; Storch, D. M. *J. Am. Chem. Soc.* **1985**, *107*, 3898.

(46) Dewar, M. J. S.; Zoebisch, E. G.; Healy, E. F.; Stewart, J. J. P. *J. Am. Chem. Soc.* **1985**, *107*, 3902.

(47) Dewar, M. J. S.; Reynolds, C. H. *J. Comput. Chem.* **1986**, *7*, 140.

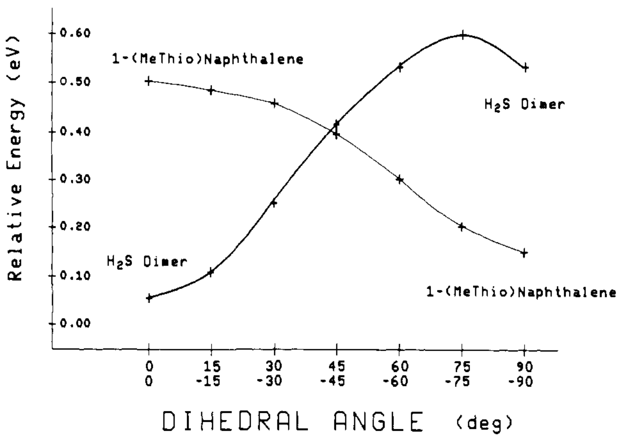

Figure 8. Dependence of the energy of the highest occupied molecular orbital of hydrogen sulfide dimer **9**, and 1-methylthionaphthalene, **10**, on C–S torsion angle as calculated by the AM1 method.

distance apart as the sulfur atoms in **5** and the S–H_a bonds were constrained such that one is colinear with the C(1)–S bond in **5** and the other with C(8)–S. The energy of the highest occupied molecular orbital of this dimer was calculated as a function of the dihedral angle between the planes of each hydrogen sulfide molecule on conrotation and disrotation around the S–H_a bonds. This calculation serves as a model for the effect of rotation about the C–S bonds of **5** on the energy of the highest occupied molecular orbital resulting solely from sulfur–sulfur lone pair interactions. The highest occupied molecular orbital of methylthionaphthalene (**10**) was calculated as a function of rotation about the C(1)–S bond. This calculation serves as a model for the effect of rotation about the C–S bonds of **5** on the energy of the highest occupied molecular orbital resulting solely from sulfur lone pair–π interactions. The results of both of these model calculations are shown in Figure 8.

The highest occupied molecular orbital of compound **5** from coplanar conformation (denoted 0,0) to antiperpendicular conformation (denoted –90, 90) obtained by conrotation about both C(1)–S and C(8)–S bonds by 90° consists of antisymmetric sulfur–sulfur p-type lone pair interactions and antibonding sulfur p-type lone pair–naphthalene π-orbital interactions according to AM1 calculations. Figure 8 shows that the antisymmetric sulfur–sulfur p-type lone pair interactions represented by dimer **9** will raise the energy of the highest occupied molecular orbital of **5** as a consequence of this rotation. However, the decreased sulfur–naphthalene antibonding interactions, represented by (methylthio)naphthalene (**10**) in Figure 8, will lower the energy of the highest occupied molecular orbital of compound **5** as a consequence of this rotation to approximately the same extent as the sulfur–sulfur interactions raise them. Thus, both interactions effectively cancel each other, rendering the first ionization potential of compound **5** essentially constant in this range.

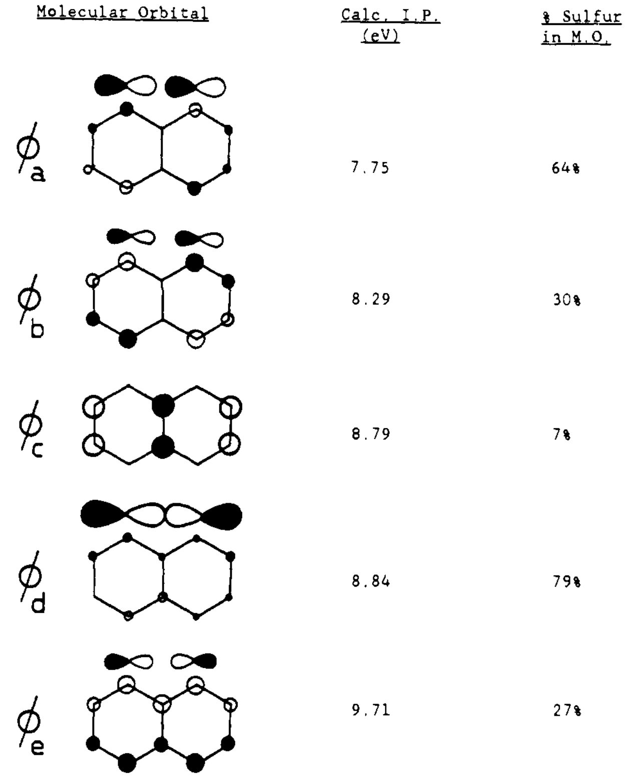

Figure 9. Orbital composition of the five highest occupied molecular orbitals for the optimized geometry of **4** as calculated by the AM1 method.

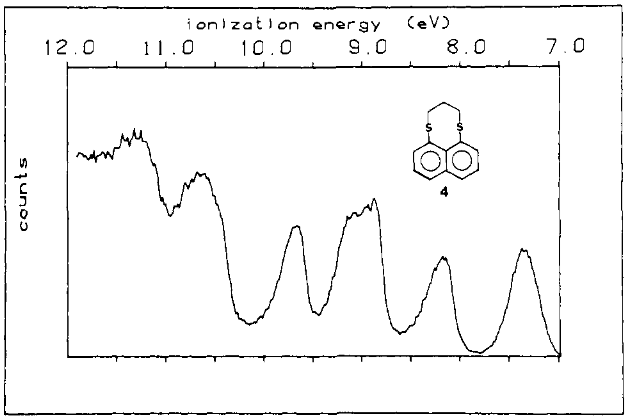

Figure 10. He I photoelectron spectrum of **4**.

Rotation in the disrotatory sense about C(1)–S and C(8)–S in compound **5** also results in little change in the value for the first ionization potential. This is due to a crossing of ϕ_1 and ϕ_2 as shown in Figure 7 at about 55° rotation. This crossing occurs because ϕ_1 is stabilized due to decreasing antibonding sulfur p-type lone pair–naphthalene π-orbital interactions and increasing symmetric sulfur–sulfur p-type lone pair interactions but ϕ_2 is strongly destabilized due to increasing antisymmetric sulfur–sulfur p-type lone pair interactions despite being weakly stabilized by decreasing antibonding sulfur–naphthalene interactions during the course of this rotation. The net effect of this crossing is a relatively constant first ionization potential on 90° disrotation of compound **5**. It should also be noted that at (90, 90) and (–90, 90) the energies and compositions of the molecular orbitals are virtually identical. This is as expected because in these two conformations the sulfur p-type lone pair orbitals are in identical positions, i.e., orthogonal to the naphthalene π-molecular orbitals. With this reasonable analysis provided by AM1, the orbital compositions for the five occupied molecular orbitals of highest energy for the optimized geometry for **4** (the geometry, optimized computationally, is similar to that in the solid state determined by X-ray crystallographic techniques, but there are important differences which will be discussed below) were then determined by AM1 and the results are presented in Figure 9. The first five ionization potentials shown in Figure 9 (7.75, 8.29, 8.79, 8.84, and 9.71 eV) were calculated from the eigenvalues of the first five HOMOs of compound **4** using the equation given in the caption of Figure 7. The photoelectron spectrum measured for **4**, shown in Figure 10, gives experimental ionization potentials of 7.35, 8.16, 8.85, 9.12, and 9.65 eV. There is reasonable correspondence between the calculated and observed spectrum although the calculated lowest ionization potential is significantly higher than the measured potential. The consequences of this inaccuracy are discussed below. In addition, in accordance with the AM1 prediction that the lowest ionization potential is independent of the torsion angle about the C–S bond, the lowest ionization potential for **4** is close to that for **5**, i.e., 7.35 and 7.42 eV (as measured by us) or 7.55 eV (as previously reported),[41,42] respectively. The sulfur–sulfur lone pair splitting can be derived from the AM1 calculations with the correlation diagram shown in Figure 11. As shown in Figure

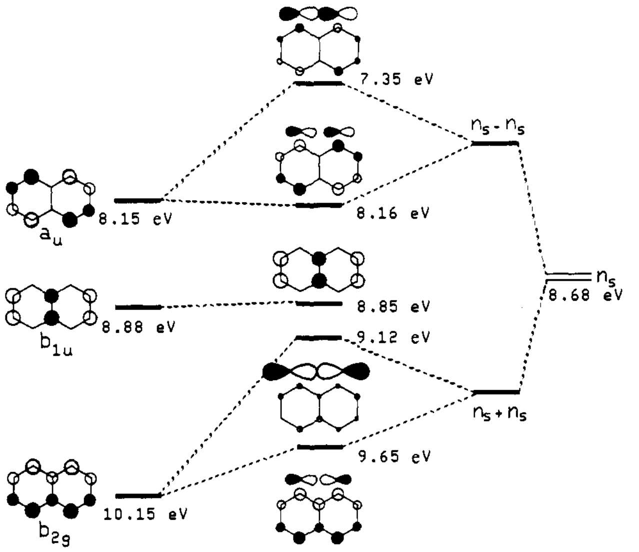

Figure 11. Correlation diagram for **4** deduced from orbital compositions determined by AM1 calculations.

11, the AM1 method reveals that molecular orbitals ϕ_a and ϕ_b are mixtures of the antisymmetric combination of the sulfur lone pair orbitals and naphthalene a_u orbital. Molecular orbitals ϕ_d and ϕ_e are mixtures of the symmetric combination of sulfur lone pair orbitals and the naphthalene b_{2g} orbital. This analysis would result in an estimation of the sulfur–sulfur lone pair splitting of 1.63 eV $\{[(9.65 + 9.12)/2] - [(8.16 + 7.35)/2]\}$. The sulfur–sulfur lone pair splitting can result in principle from through-bond or through-space effects.[11,28,48] Indeed it has been shown that both effects are important in the interaction between the triple bonds in diyne **11**.[49] The AM1 calculations on **4** show that through-space effects predominate except for the fifth highest occupied molecular orbital (ϕ_e) in which there are significant contributions from the carbon atoms of the $(CH_2)_3$ moiety bridging the sulfur atoms. These contributions have been left out of Figure 9 for simplicity, but their contributions should not be overlooked because they represent antisymmetric through-bond interaction between the sulfur p orbitals analogous to that of the acetylene π-orbitals identified in diyne **11**.[49]

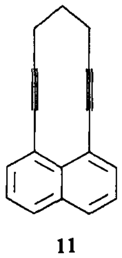

11

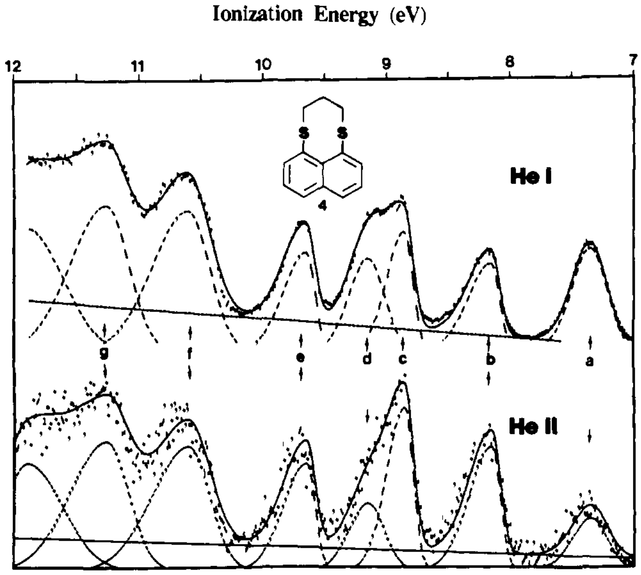

Figure 12. Comparison of the He I and He II photoelectron spectra of **4**.

Table VIII. He I and He II Photoelectron Spectral Data of Compound **4**

band	IP, eV	relative area He I	relative area He II	relative area change, percent
a	7.35	1.13	0.42	-63
b	8.16	0.87	0.90	+4
c	8.85	1.00	1.00	0
d	9.12	1.03	0.54	-47
e	9.65	0.99	0.78	-21

As illustrated above, each of the semiempirical methods used gives substantially different results in describing the five highest occupied molecular orbitals of **4**. Although AM1 calculations were anticipated to be the most reliable for the reasons outlined above and provide a reasonable fit of the experimental data, further experimental support for these calculations was sought by using a recently developed photoelectron spectroscopic method.[50] Comparison of He I and He II photoelectron spectra has been shown to be a reliable method for determining the sulfur 3p and carbon π-orbital composition of molecular orbitals. The intensity of ionizations from a sulfur p-type orbital decreases 60–70% relative to ionizations from a carbon π-molecular orbital on changing the ionizing source from He I to He II. Thus, the sulfur 3p and naphthalene π-orbital compositions of the molecular orbitals of **4** can be ascertained. Since these compositions differ depending on the computational method, independent experimental discrimination among these calculations is at hand. The He I and He II spectra for compound **4** are compared in Figure 12 and Table VIII. As shown in the table, the intensity of bands b and c show essentially no change on going from He I to He II sources relative to each other, but bands a, d, and e markedly decrease in relative area. AM1 calculations show that band c is essentially a pure naphthalene π-molecular orbital very similar to the b_{1u} orbital in naphthalene. Furthermore, the measured ionization potential for band c in compound **4** is 8.85 eV, which is almost identical with that for the b_{1u} orbital in naphthalene (8.88 eV). Hence, band b, which does not change in relative area compared to band c, must be due to ionization from the a_u naphthalene π-molecular orbital with little sulfur p orbital character. On the other hand, band a must correspond to ionization from a molecular orbital with only sulfur p orbital contribution. The relatively lower decrease in intensities of bands d and e suggest ionizations from molecular orbitals composed of both sulfur 3p and carbon π-orbitals (proportionately more of the former than the latter for the molecular orbital corresponding to band d and vice versa for band e). These results are more consistent with the AM1 than the other calculations. The AM1 assignments for bands c–e are in agreement with the experimental results, but these calculations suggest more mixing of the a_u orbital of naphthalene and the antisymmetric combination of the sulfur p orbitals to form molecular orbitals ϕ_a and ϕ_b as shown in the correlation diagram given in Figure 11. The source of the disagreement between experiment and AM1 calculations may be due to the difference in the calculated and experimental lowest ionization potential for compound **4**. The AM1 calculations predict an ionization potential of 7.75 eV, but the experimental result is 7.35 eV. This lowering in energy of molecular orbital ϕ_a by AM1 compared to the experimental result allows more mixing to occur between ϕ_a and ϕ_b because they would be closer in energy. With use of the experimental result that ϕ_a is essentially composed of lone-pair orbitals and ϕ_d and

---

(48) Heilbronner, E.; Maier, J. P. In *Electron Spectroscopy: Theory Techniques and Applications*; Bundle, C. R., Baker, A. D., Eds.; Academic: New York, 1977; Vol. 1, Chapter 5.

(49) Gleiter, R.; Schäfer, W.; Flatow, A. *J. Org. Chem.* **1984**, *49*, 372.

(50) Glass, R. S.; Broeker, J. L.; Jatcko, M. E. Submitted for publication.

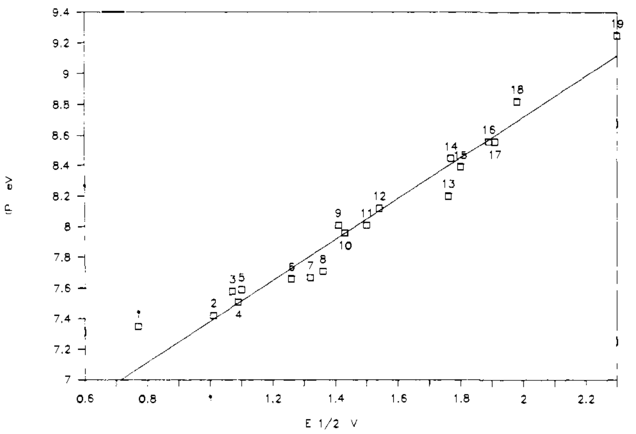

Figure 13. Correlation of first half-wave oxidation potential ($E_{1/2}$), in V versus SCE, with lowest energy ionization potential (IP), in eV, for (1) naphtho[1,8-*b,c*]-1,5-dithiocin,[a] (2) 1,8-bis(methylthio)naphthalene,[a] (3) 1,4-bis(methylthio)naphthalene,[b,e] (4) anthracene,[b,c] (5) 2,6-bis(methylthio)naphthalene,[b,e] (6) 1,5-bis(methylthio)naphthalene,[b,e] (7) 1-(methylthio)naphthalene,[b,e] (8) 2-(methylthio)naphthalene,[b,e] (9) thioanisole,[d,e] (10) 1-methylnaphthalene,[c] (11) phenanthrene,[c] (12) naphthalene,[c] (13) anisole,[c,e] (14) *p*-xylene,[c] (15) mesitylene,[c] (16) *o*-xylene,[c] (17) *m*-xylene,[c] (18) toluene,[c] (19) benzene.[c] ([a]*This* work with E_p values used instead of $E_{1/2}$ values. [b]*Reference* 12. [c]*Reference* 56. [d]*Reference* 57. [e]*Reference* 41.)

ϕ_e are composed of both sulfur 3p and carbon π-orbitals, the sulfur–sulfur lone pair splitting would be approximately 2 eV {[(9.65 + 9.12)/2] − 7.35}. Clearly this splitting is of unprecedented magnitude and substantially greater than that in 1,5-dithiocane (0.4 eV) albeit significantly less than that calculated by CNDO methods. The basis for this enormous splitting compared with 1,5-dithiocane is due to their differences in geometry. The sulfur atoms are held closer together in **4** (the S···S nonbonded distance in **4** is 3.23 Å in the solid state and is estimated to be 3.4 Å in 1,5-dithiocane) and the p-type orbitals on the sulfur atoms in **4** point almost directly at each other, but they are somewhat askew in 1,5-dithiocane. These two geometrical features result in far greater overlap of the p-type orbitals on each of the sulfur atoms in **4** than in 1,5-dithiocane, resulting in increased transannular interaction.

The consequence of this enormous interaction in **4** is an unusually low first ionization potential of 7.35 eV. Ordinary thioethers have much higher first ionization potentials[28,51] (the first ionization potential of dimethyl sulfide is 8.65–8.68 eV[52,53]) as does naphthalene, whose first ionization potential is 8.15 eV.[54] It was of great interest to determine if this unusually low first ionization potential for **4** would result in exceptional redox chemistry. Consequently, the redox chemistry of **4** was studied by electrochemical methods as outlined below.

Electrochemical Studies. Cyclic voltammetric studies of **5** show irreversible oxidation in acetonitrile with a peak potential of +0.70 V versus Ag/0.1 M $AgNO_3$ in acetonitrile reference electrode. Correcting this result to an aqueous SCE reference[55] gave a value of about 1.0 V, which is in good agreement with the previously reported result of 1.09 V.[12]

Linear correlation between the polarographic oxidation half-wave potentials for aromatic compounds and their ionization potentials have been reported by Pysh and Yang.[56] Compound **5** and other methylthio and bis(methylthio)naphthalenes[41] and thioanisole[41,57] fit this correlation as shown in Figure 13. The equation for the least-squares line shown in Figure 13 is IP (eV) = (1.336)($E_{1/2}$, *V*) + 6.045.

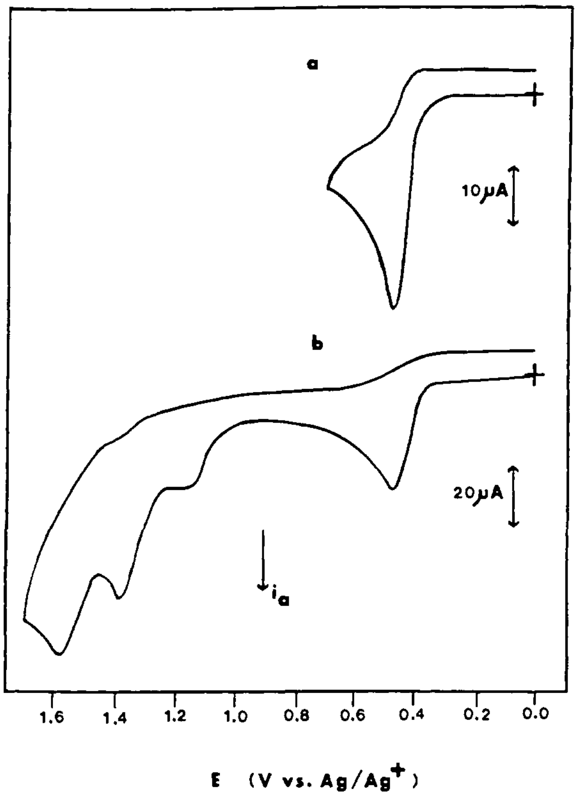

Figure 14. Cyclic voltammogram of **4** determined at a Pt electrode, 0.1 V/s scan rate, and measured in acetonitrile, 0.1 M in lithium perchlorate, versus Ag/0.1 M $AgNO_3$ in acetonitrile reference electrode: (a) cyclic scan in the range 0–0.7 V beginning at 0 V and (b) cyclic scan in the range 0–1.7 V beginning at 0 V.

The cyclic voltammogram of **4** is shown in Figure 14. The first oxidation has a peak potential of 0.47 V versus a Ag/0.1 M $AgNO_3$ in acetonitrile reference electrode and shows no reversible behavior with cyclic scan rates of up to 500 mV/s. Examination of the peak current dependence on scan rate in the range 10–200 mV/s demonstrates diffusion control for this process. As shown in Figure 14, scanning to higher potentials reveals three more anodic waves at 1.15, 1.35, and 1.58 V. These peaks are also observed in the cyclic voltammogram of naphtho[1,8-*b,c*]-1,5-dithiocin 1-oxide, **12**. Since this compound is the product of oxidation of **4**, these peaks in the cyclic voltammogram of **4** are ascribed to the oxidation of **12**. Controlled-potential electrolysis of **4** at an applied potential of 0.6 V resulted in the passage of 1.8 equiv of charge before the current decayed to zero. The product was isolated by TLC in 80% yield (95% current yield) and shown to be identical with authentic **12**.[58] Formation of sulfoxide **12** on the electrochemical oxidation of **4** is consistent with removal of an electron from the highest occupied molecular orbital which is sulfur lone pair in character followed by attack by water at sulfur.

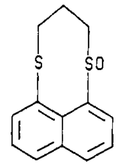

12

---

(51) Glass, R. S.; Wilson, G. S.; Coleman, B. R.; Setzer, W. N.; Prabhu, U. D. G. *Adv. Chem. Ser.* **1982**, *201*, 417.

(52) Frost, D. C.; Herring, F. G.; Katrib, A.; McDowell, C. A.; McLean, R. A. N. *J. Phys. Chem.* **1972**, *76*, 1030.

(53) Cullen, W. R.; Frost, D. C.; Vroom, D. A. *Inorg. Chem.* **1969**, *8*, 1803. Cradock, S.; Whiteford, R. A. *J. Chem. Soc., Faraday Trans. 2* **1972**, *68*, 281. Bock, H.; Wagner, G. *Angew. Chem., Int. Ed. Engl.* **1972**, *11*, 150. Wagner, G.; Bock, H. *Chem. Ber.* **1977**, *107*, 68.

(54) Bock, H.; Wagner, G.; Kroner, J. *Chem. Ber.* **1972**, *105*, 3850.

(55) Yoshida, Z. *Electrooxidation in Organic Chemistry*; Wiley: New York, 1984; p 32.

(56) Pysh, E. S.; Yang, N. C. *J. Am. Chem. Soc.* **1963**, *85*, 2124.

(57) Meites, L.; Zuman, P. In *Electrochemical Data*, Part 1; Wiley: New York, 1974; Vol. A, p 292.

(58) Authentic **13** was prepared by oxidation of **4** with sodium metaperiodate. Its preparation and full characterization will be reported elsewhere.

The peak potential for oxidation of **4** is lower than that for **5** as expected owing to the lower first ionization potential for **4** than for **5** (7.35 eV versus 7.42 eV). However, the oxidation potential and ionization potential for **4** do not linearly correlate with those of other aromatic compounds as shown in Figure 13. This result is not unexpected since the lowest ionization potential for **4** corresponds to removal of an electron from a sulfur lone pair orbital not a π-molecular orbital and, therefore, it is more appropriate to correlate the data for **4** with that for aliphatic thioethers. A linear correlation of ionization potentials with peak potentials has been reported[51] for aliphatic sulfur compounds except for those with "isolated" aliphatic sulfur, where neighboring-group participation is either not likely or not possible. However, the data for **4** do not correlate with this group of compounds. To exemplify this point, compare the data for **4** with that for 1,5-dithiocane which fits this correlation.[51] The lowest ionization potential for **4** is 0.95 eV lower (7.35 eV versus 8.30 eV) than that for 1,5-dithiocane, but its peak potential is 130 mV more positive (0.47 V versus 0.34 V). This suggests that neighboring-group participation in **4** on oxidation is less effective than in 1,5-dithiocane. Such participation has been suggested previously[51] as dominant in the overall electron-transfer energetics, making the solvent reorganization contribution relatively unimportant and leading to outer sphere electron transfer. Under such conditions good correlation between peak potential and ionization potential is expected. The electrochemical results shown in Figure 14 also indicate that the radical cation and dication of **4** are much less stable than the corresponding species of 1,5-dithiocane. This is consistent with the observation that anodic oxidation of **4** is irreversible under conditions in which 1,5-dithiocane oxidizes reversibly. Attack by residual water in the acetonitrile solvent on the radical cation and/or dication of **4** rendering oxidation of **4** irreversible is faster than on the corresponding species of 1,5-dithiocane, perhaps due to weaker bonds in the former species compared to the latter. Analogous correlations between the bond strengths of two-center three-electron bonded thioether radical cations with the deprotonation kinetics of these species has been reported.[59] However, it is not obvious why the radical cation of **4** is relatively unstable. Geometric factors should enhance the stability of this species. Gill and Radom[60] recently found the S–S bond distance in $(H_2S)_2^{\bullet+}$ to be 2.835 Å by ab initio calculations at the MP2/6-31G* level. Furthermore, the distance between the 1,8-peri positions in naphthalene itself is 2.4–2.5 Å[10] and an S–S bond can be formed easily between sulfur atoms in these positions as exemplified by naphtho[1,8-*c,d*]-1,2-dithiole.[12] Consequently, bringing the sulfur atoms into optimal bonding distance in the radical cation from that in **4** itself (3.23 Å in the solid state) should be favorable.

Conclusions

The molecular constraints in naphtho[1,8-*b,c*]-1,5-dithiocin, **4**, result in close juxtaposition of the two sulfur atoms with the p-type lone pair orbitals on each of the sulfur atoms directed almost at each other and nearly orthogonal to the naphthalene π-system. These factors result in an unprecedentedly large lone pair–lone pair splitting of the sulfur p-type orbitals of 1.6–2.0 eV. The AM1 method provides reasonable agreement with the experimentally measured He I and He II photoelectron spectra of **4** and is the method of choice for semiempirical calculations on such systems. This method predicts that the energy of the highest occupied molecular orbital in 1,8-bis(methylthio)naphthalene is essentially independent of the C(1)–S and C(8)–S torsion angles and this is supported by the similar lowest ionization potentials for **4** and **5**. This provides a measure of confidence in the rationale, provided by AM1 calculations on model systems, of compensating effects on such rotation. The electrochemical studies on **4** support the conclusion that its highest occupied molecular orbital consists essentially of sulfur lone pair character, but the exceptionally low first ionization potential compared with aliphatic thioethers does not manifest itself in an exceptionally low anodic peak potential compared with 1,5-dithiocane probably because the oxidation is irreversible.

Table IX. Crystal Data[a] for **4**

mol formula	$C_{13}H_{12}S_2$
mol wt	232.37
space group	*Pbca*
a, Å	8.140 (2)[b]
b, Å	9.866 (1)[b]
c, Å	28.302 (3)[b]
Z	8
d_{calcd}, g cm^{-3}	1.36
cryst color, shape	yellow, irregular
cryst dimens, mm	0.30 × 0.20 × 0.10
radiation, Å	λ(Mo Kα) 0.71073
monochromator	graphite cryst
no. of unique data	1996
no. of obsd data	1169
abs coeff [$\mu(\lambda)$], cm^{-1}	4.12
R	0.046
R_w	0.049
GOF	1.82

[a] The numbers in parentheses are estimated standard deviations in the least significant digits. [b] The cell dimensions were obtained from a least-squares refinement of setting angles of 25 reflections in the 2θ range of 20–50°.

Experimental Section

Naphtho[1,8-*b*,*c*]-1,5-dithiocin (4). To a two-phase mixture degassed with argon and prepared by adding aqueous sodium hydroxide solution (3.7 *N*, 10 mL, 37 mequiv) to a 40% (v/v) solution of aqueous tetrahydrofuran (55 mL) were added naphtho[1,8-*c,d*]-1,2-dithiole (100 mg, 0.53 mmol),[12] aminoiminomethanesulfinic acid (102 mg, 0.94 mmol), and cetyltrimethylammonium bromide (20 mg, 0.05 mmol) successively in analogy with the procedure of Ferreira et al.[15] To this mixture stirred and heated under reflux in a three-necked round-bottom flask equipped with a reflux condenser, pressure-equilibrating addition funnel, and an inert-gas inlet was added a degassed solution of 1,3-dibromopropane (106 mg, 0.53 mmol) in tetrahydrofuran (15 mL) dropwise (5–10 drops/min). Two more portions (2 × 100 mg) of aminoiminomethanesulfinic acid were also added during the course of the addition of the dibromide to ensure complete reduction of the disulfide. After completion of the addition, the mixture was stirred and heated at reflux for 1 h. At the end of this time, the original red-orange color was replaced by yellow-green. After the mixture cooled to room temperature, the tetrahydrofuran layer was separated by use of a separatory funnel and the aqueous layer was extracted with additional tetrahydrofuran (3 × 30 mL). The tetrahydrofuran layers were combined and concentrated by rotary evaporation until a yellow precipitate began to form. The mixture thus obtained was extracted with chloroform (5 × 50 mL) and the combined extracts were dried ($MgSO_4$), filtered, and concentrated with a rotary evaporator to a bright yellow solid. This solid was purified by preparative TLC on silica gel by eluting with 30% dichloromethane in hexanes to afford yellow, crystalline **4**: 104 mg (85% yield); mp 82 °C; IR (KBr) 1430, 1315, 1202, 1010, 910, 825, 763 cm^{-1}; ^{1}H NMR ($CDCl_3$, 250 MHz) δ 1.85 (m, 2 H, CCH_2), 3.02 (t, *J* = 6 Hz, CH_2S), 7.38 (dd, *J* = 8, 8 Hz, 3,6-ArH), 7.75 (dd, *J* = 8, 1 Hz, 2,7-ArH), 7.97 (dd, *J* = 8, 1 Hz, 4,5-ArH); UV (95% EtOH) λ_m 227 (4700), 290 (4700), 372 (1800) nm; MS *m/z* calcd for $C_{13}H_{12}S_2$ 232.0380, found 232.0379.

1,8-Bis(methylthio)naphthalene (5). This known[12] compound was obtained as a yellow solid after recrystallization from diethyl ether–pentane: mp 83–85 °C; IR (KBr) 2930, 1420, 1196, 819, 761 cm^{-1}; ^{1}H NMR ($CDCl_3$, 250 MHz) δ 2.53 (s, 6 H, CH_3), 7.36 (dd, *J* = 7.7, 7.7 Hz, 2 H, 3,6-ArH), 7.48 (dd, *J* = 7.4, 1.2 Hz, 2 H, 2,7-ArH), 7.64 (dd, *J* = 8.0, 1.3 Hz, 4,5-ArH).

X-ray Single-Crystal Structure Study of 4. A yellow, irregular crystal (0.30 × 0.20 × 0.10 mm) was grown by vapor diffusion of pentane into a concentrated solution of **4** in diethyl ether and mounted on a glass fiber in a random orientation on a Syntex P2$_1$ autodiffractometer. The automatic centering and least-squares routines were carried out on 25 reflections in the range 20° < 2θ < 50°, and the cell constants determined by least-squares refinement of these reflections are given in Table IX. The orthorhombic space group was uniquely determined from systematic absences to be *Pbca* (No. 61). The ω data collection technique was used, and data were collected to a maximum 2θ of 50.0°. The data with $F \geq 3\sigma(F)$ were used in the calculations. The data were reduced to F_o and $\sigma(F_o)$. Lorentz and polarization corrections were applied to the data.

---

(59) Mönig, J.; Goslich, R.; Asmus, K.-D. *Ber. Bunsenges. Phys. Chem.* **1986**, *90*, 115.

(60) Gill, P. M. W.; Radom, L. *J. Am. Chem. Soc.* **1988**, *110*, 4931.

Table X. Crystal Data[a] for **5**

mol formula	$C_{12}H_{12}S_2$
mol wt	220.25
space group	$P\bar{1}$
a, Å	8.257 (2)[b]
b, Å	12.079 (3)[b]
c, Å	12.157 (2)[b]
α, deg	87.87 (2)[b]
β, deg	72.72 (2)[b]
γ, deg	74.16 (2)[b]
Z	4
d_{calcd}, g cm^{-3}	1.32
d_{obsd}, g cm^{-3}	1.31[c]
cryst color, shape	yellow, plates
cryst dimens, mm	0.30 × 0.33 × 0.23
radiation, Å	λ(Mo Kα)0.71073
monochromator	graphite cryst
no. of unique data	2882
no. of obsd data	2671
abs coeff [$\mu(\lambda)$], cm^{-1}	4.17
R	0.077
R_w	0.109
GOF	3.180

[a] The numbers in parentheses are estimated standard deviations in the least significant digits. [b] The cell dimensions were obtained from a least-squares refinement of setting angles of 25 reflections in the 2θ range of 20–30°. [c] The density was determined by the flotation method using aqueous potassium iodide solution.

Three standards monitored every 97 reflections indicated no decay.

The structure was solved by direct methods using the SDP-PLUS program package.[61] With default parameters, a total of 12 atoms were located. The remaining atoms including hydrogen atoms were located in difference maps. The hydrogen atoms were included at idealized positions and were not refined. They were restrained to ride on the carbon atoms to which they are attached in subsequent refinements. The structure was refined by full-matrix least-squares techniques[61] by using neutral atom scattering factors[62] with anomalous dispersion terms[63] included for all atoms. The final cycle of refinement included 136 variable parameters and yielded unweighted (R) and weighted (R_w) agreement factors of 0.046 and 0.049, respectively. The standard deviation of an observation of unit weight was 1.82.

X-ray Single-Crystal Structure Study of 5. A yellow plate (0.40 × 0.33 × 0.23 mm) was grown by vapor diffusion of pentane into a concentrated solution of **5** in diethyl ether and mounted on a glass fiber in a random orientation on a Syntex P2$_1$ autodiffractometer. The automatic centering and least-squares routines were carried out on 25 reflections in the range 20° $< 2\theta <$ 30°, and the cell constants determined by least-squares refinement of these reflections are given in Table X. From subsequent least-squares refinement the triclinic space group was determined to be $P1$ (No. 2). The $\theta - 2\theta$ data collection technique was used, and the data were collected to a maximum 2θ of 50.0°. The data with $F \geq 3\sigma(F)$ were used in the calculations. The data were reduced to F_o and $\sigma(F_o)$. Lorentz and polarization corrections were applied to the data. Three standards monitored every 46 reflections indicated no decay.

The structure was solved by direct methods using the SDP-PLUS program package.[61] With default parameters, a total of 23 atoms were located. The remaining atoms including hydrogen atoms were located in difference maps. The hydrogen atoms were included at idealized positions and were not refined. They were constrained to ride on the carbon atoms to which they are attached in subsequent refinements. The structure was refined by full-matrix least-squares techniques[61] by using neutral atom scattering factors[62] with anomalous dispersion terms[63] included for all atoms. The final cycle of refinement included 253 variable parameters and yielded unweighted (R) and weighted (R_w) agreement factors of 0.082 and 0.127, respectively. The standard deviation of an observation of unit weight was 3.729. Plots of $\sum w(|F_o| - |F_c|)^2$ versus $|F_o|$, reflection order in data collection, sin θ/λ, and various classes of indices showed five reflections with W*DEL**2 > 1000. These five reflections were removed and an additional cycle of least-squares was run. With 2671 reflections and 253 variable parameters, this refinement gave weighted (R) and weighted (R_w) agreement factors of 0.077 and 0.109, respectively. The standard deviation of an observation of unit weight was 3.180. There was no movement of any of the parameters, no change in the difference maps, and no change in the correlation coefficients.

Cyclic Voltammetry. Voltammograms were measured on solutions approximately 10^{-3} M in compound **4** or **5** and 0.1 M in lithium perchlorate, which served as supporting electrolyte, in acetonitrile with a Ag/0.1 M $AgNO_3$ in acetonitrile reference electrode. A 0.3-cm^2 platinum flag, which was heated to incandescence in a flame prior to each run, served as the working electrode, and the data were collected with a cyclic scan rate of 0.1 V/s. The electrochemical apparatus was purged with nitrogen, and the experiment was run under a nitrogen atmosphere. The electrochemical instrumentation, data acquisition, and data processing systems have been described.[64]

Controlled-Potential Electrolysis of 4. A sample of **4** (19 mg, 0.082 mmol) dissolved in acetonitrile 0.1 M in lithium perchlorate was exhaustively electrolyzed at a constant potential of 0.6 V versus a Ag/0.1 M $AgNO_3$ in acetonitrile reference electrode. When the current decayed to 0.1% of its initial value, 14.22 C had passed corresponding to an "n" value of 1.8. This solution was concentrated to near dryness and, after preparative TLC on silica gel by eluting with ethyl acetate, sulfoxide **12** was obtained as a solid (17.8 mg) in 80% yield: mp 80–81° C, identical with authentic compound by mp, IR and ^{1}H NMR spectroscopy, and TLC behavior.

Acknowledgment. We gratefully acknowledge support of this work by the U.S. Public Health Service, National Institutes of Health, Grant No. HL 15104. The photoelectron spectra reported in this paper were measured in the Laboratory for Electron Spectroscopy and Surface Analysis of the Department of Chemistry, The University of Arizona, and we thank Mark E. Jatcko for assistance in obtaining these spectra. We also thank Dr. Michael A. Bruck and the Molecular Structure Laboratory of The University of Arizona for use of the X-ray and computational facilities and assistance during the crystal structure analyses.

Supplementary Material Available: General experimental section, including photoelectron spectroscopic methodology, stereoscopic view of the packing of the molecules in the unit cell of **4** and **5**, and tables of final atomic positional and thermal parameters (13 pages) (a listing of structure factor amplitudes is available from the authors). Ordering information is given on any current masthead page.

---

(61) All calculations were performed on a PDP-11/34 computer using SDP-PLUS: Frenz, B. A. In *Computing in Crystallography*; Schenk, H., Olthof-Hazelkamp, R., von Konigsveld, R., Bassi, G. C., Eds.; Delft University: Delft, Holland, 1978; pp 64–71.

(62) Cromer, D. T.; Waber, J. T. *International Tables for X-ray Crystallography*; Kynoch: Birmingham, England, 1974; Vol. IV, Table 2.2B.

(63) Ibers, J. A.; Hamilton, W. C. *Acta Crystallogr.* **1964**, *17*, 781.

(64) Langhus, D. L.; Wilson, G. S. *Anal. Chem.* **1979**, *51*, 1139.

(65) Johnson, C. K. ORTEP; Oak Ridge National Laboratory: Oak Ridge, TN, 1965.